Current and Speed Control Operating Modes of a Reaction Wheel

VALDEMIR Carrara[1,a*] and HELIO Koiti Kuga[1,b]

[1]Instituto Nacional de Pesquisas Espaciais – INPE – Av. dos Astronautas, 1758, São José dos Campos, CEP 12227-010, SP – Brazil

[a]valdemir.carrara@inpe.br, [b]helio.kuga@inpe.br

Abstract. This paper presents some approaches to the design and some experimental results for current and speed control loops of a reaction wheel (RW). Reaction wheels are largely employed in satellite attitude control due to its large range of torque capability, small power consumption and high reliability. However, to achieve such performance the RW design shall deal with several restrictions, such as to support the space environment hazards (radiation, vacuum, high and fast temperature variation), and launch requirements (vibration, noise and choke). In this work some experimental results of an air-bearing table attitude control equipped with a Fiber Optics Gyro (FOG), a reaction wheel and a small fan will be presented. The RW is controlled by speed reference, and a second speed mode control similar to the first one was implemented in an external computer. Both were then compared by means of the air-bearing attitude control performance during the wheel zero-speed crossing. The results showed that the controllers have similar performance, as expected, and the maximum attitude pointing error remained below 0.08 degrees, which complies with the attitude requirements of Earth pointing satellites.

Introduction

With increasing access to space via satellites, several nations now are engaged to gain knowledge in the development and manufacture of qualified components to equip their own satellites. Among these components, the Attitude Control System (ACS) shall be pointed out, which often represent a significant portion of the satellite cost. The ACS ranges from the simplest ones (and usually with low pointing precision, low cost and low reliability) to more sophisticated ones, which consists of dozens of devices with their own electronic and interfaces. The ACS system is mostly composed of sensors, actuators and control electronics or on-board computer. Almost all sensors and actuators rely solely in electronics to properly work, but some have moving parts that can present wear and aging malfunction in the space environment. Examples of these equipments are the scanning horizon sensor (barely used in today satellites), cold or hot gas thrusters and their valves, reaction wheels (RW) and momentum wheels (MW - sometimes also named as flywheels). The latter are composed of a high inertia rotor coupled to a brushless DC motor (BLDC motor). They provide attitude control by exchanging angular momentum with the space vehicle. Although the cost of the reaction and momentum wheels is constantly decreasing, the manufacturing complexity and especially their required reliability make them still expensive. Currently RW are required for satellites ranging from few pounds to several tons. The main challenges in its construction are the bearing design, bearing lubrication, assembly sealing and motor control electronics. Performance requirements introduce several additional constraints, such as low power, low mass, small volume and high reliability, among others.

It is well known the fact that the friction in the bearings modifies the behaviour of the wheels so their performance is compromised. In fact, the static friction delays the motor to start till the stator current reaches a certain threshold [1], introducing a dead zone operation around the zero-speed or when the wheel reverses its rotation sense. This dead zone causes a noticeable error in the pointing attitude, sometimes large enough to exceed the maximum required attitude deviation during wheel reversions.

A RW normally can operate in two different modes: Current and Speed Control Modes, shown in Fig. 1. In a DC motor the torque is approximately proportional to the electric current in the stator. By measuring the current, an analog or sometimes digital closed loop controller controls the torque. This is the Current Control loop. In order to avoid the disagreement between current command and torque response, due to the non-linear friction torques, the wheels are also equipped with a angular rate control loop, that adjusts the current in order to make the wheel to follow a given reference angular speed. This control is called Speed Control Mode, in contrast to the Current Control. Since the angular acceleration of the wheel is linked to the net torque (the difference between the motor torque and the friction torques), by measuring the acceleration some commercial RWs can operate also in a Torque Control Mode.
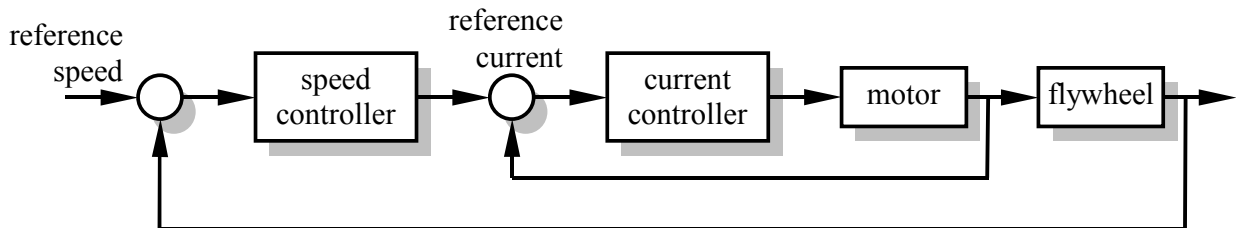

Figure 1: Current and Speed Control Modes of a Reaction Wheel.

Because aspects involving the reaction wheel technology have commercial appeal, only a small number of academic papers report RW design details or performance tests. While several papers deal with models of friction in ball bearings or a general BLDC electronic drive, few can be associated with the wheel design. In fact, a significant parcel of BLDC motor applications in the industry is associated with servomotors for robotics or machine tools. In the first case, the precise position control is the focus rather than velocity, and, in the second case, the operation is generally done at high speeds, whatever it may be. A reaction wheel, in contrast, must operate at peak performance in a precise angular velocity, ranging from zero to plus or minus an upper limit.

In [2] the friction parameters of a reaction wheel commanded in current are raised from experimental means and calculated by curve fitting, based on minimum quadratic variation, and took into account the Coulomb and viscous frictions. In [3] a DMC (Dynamic Model Compensator) of the non-linear friction was used to control the attitude of the air-bearing table. The DMC decreased by one order of magnitude the attitude error during wheel reversing when compared to the normal current control mode. Later the control modes, current and speed, were compared in [4], which showed that the DMC introduces an error comparable but slightly higher to the speed control mode.

Few works in the literature relate friction models with reaction wheels bearings [5, 6]. On the other hand, several papers present friction models and estimation of parameters in rotors, as in [7] and [8], including a friction dynamic model [9, 10], based on the LuGre (Lund-Grenoble) friction model [11]. This last model was later employed in [12] to estimate the parameters of a reaction wheel by Kalman filtering. A model of the slip-stick phenomenon was simulated in [13], while [14] presented a dynamic model based on the generalized Maxwell-slip friction. In [15] it is proposed a dynamic controller for system with a bristle model for non-linear friction effects. In [6] it is shown a simulation of a satellite attitude control including the RW with the LuGre friction model, for both the current and the speed control modes, and concluded that the speed controller is better than the current controller. A simulation of a RW designed for Cubesats is presented in [16].

The National Institute for Space Research (INPE) of Brazil started a development program of reaction wheels for small satellites, supported by the SIA (Inertial Systems for Aerospace Applications) project, which aims to reach an engineering model in the next few years. Several Brazilian universities and technology institutions are involved in this program. In order to increase the technological knowledge base of reaction wheels, their operation modes, electronic circuitry and

bearing friction have been studied and analysed, so as to have a mathematical model not only for the wheel dynamics, but also to serve as a guide line of the motor controller design and development.

In this direction, the work presented here will describe an external speed control loop implemented in an off-the-shelf reaction wheel, and some comparisons of this control with its built-in speed control. The experiments will be conducted using an single axis air bearing table equipped with the RW, a FOG (Fiber Optics Gyro), a RW/FOG electronic control, a wireless modem for telemetry and remote command, a power supply battery and a computer fan used to generate a disturbance attitude torque, all shown in Fig. 2. Fig. 3 presents the block diagram of the air bearing attitude controller. This arrangement differs from a satellite attitude controller since it has a single control axis while the satellite must control its attitude in all 3 axes. Moreover, the satellite attitude control relies on several sensors, like gyroscopes, star tracker, magnetometer and solar sensors, and also several actuators, like thrust gas jets, magnetic coils and reaction wheels, of course. A customized on-board computer provides the control laws, attitude operating modes, sensor readings, actuator commanding, and also send the attitude data to the telemetry subsystem, in order to resend it to ground, and decodes the received ground commands.
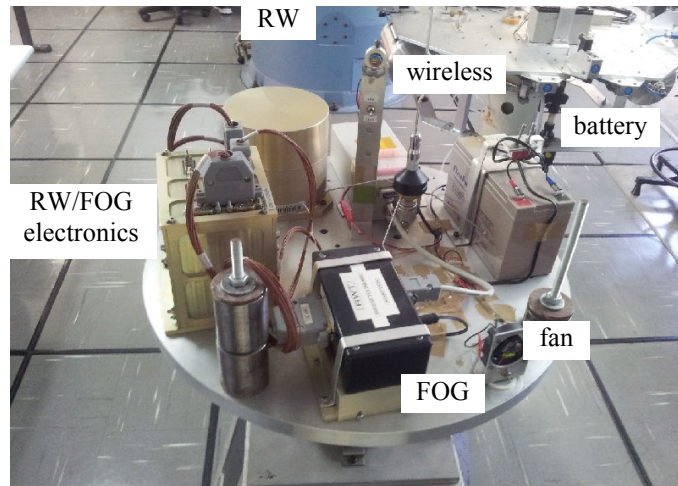

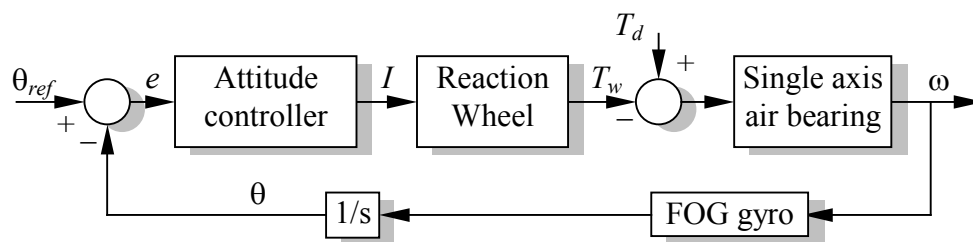Figure 2: Single axis air bearing table with the RW and the FOG gyro.

Figure 3: Block diagram of the air bearing attitude controller.

An attitude controller based on the pointing error, provided by the integral signal of the gyroscope, was implemented on an off-platform computer, which communicates with the control electronics via serial wireless modem. The wireless link is necessary since any cabling for communication between the table and the attitude controller introduces a large and unacceptable torque. However, the time lag of communication protocol conversion from RS422 to RS232 to USB and its influence on the controller shall be verified by further analysis. The external speed control loop will also be performed on the computer, and will rely on the telemetry information of the wheel's speed rate. The output response of this wheel will be reported for both the external and internal speed mode control loops. Finally, these two controllers will be compared by means of the air-bearing table attitude error when the wheel is forced to reverse its sense of rotation in response to the action of the fan.

Next Section will describe the dynamic and kinematical models of both the table and the reaction wheel, together with its block diagram. Then the RW speed controllers will be presented while the air-bearing attitude control is shown afterwards. The experimental results are shown at the end, followed by the conclusions.

Kinematics and dynamic models

The single axis air-bearing table can be modeled as an inertia subject to the disturbance torque and the reaction wheel torque. The dynamic equation for a single axis motion is then given by

$$J_p \, \dot{\omega} = T_d - T_w, \tag{1}$$

where J_p is the platform inertia around the vertical axis, ω is the table angular rate, as measured by the gyroscope, T_d is the disturbance torque and T_w is the wheel's reaction torque, given by the difference between the motor and the wheel's friction torques. On the other side, by applying the angular momentum law to the flywheel it has

$$J_w \, (\dot{\omega} + \dot{\omega}_w) = T_w, \tag{2}$$

in which ω_w is the wheel's angular rate relative to the air-bearing table and J_w is the wheel inertia, including the rotor and any rotating mass attached to the wheel. In previous works [2, 3] the air bearing residual viscous friction was estimated, and proven to be neglected provided the angular rate of the bearing remains small. So the air-bearing table and wheel dynamic equations can be manipulated as to result in

$$\dot{\omega} = \frac{T_d}{J_p} - \frac{T_w}{J_p}, \tag{3}$$

and

$$\dot{\omega}_w = \frac{T_w}{J_r} - \frac{T_d}{J_p}, \tag{4}$$

where the mean inertia J_r is defined by

$$J_r = \frac{J_p J_w}{J}, \tag{5}$$

and J is the total platform moment of inertia around the rotation axis ($J = J_p + J_w$). The dynamic equations can be solved numerically or analytically if both the disturbance and the reaction torques are known. Assuming that a viscous linear torque plus a constant Coulomb torque compose the wheel's bearing friction, then the reaction torque can be modelled [4, 17] as:

$$T_w = T_m - b \, \omega_w - c \, \text{sgn}(\omega_w), \tag{6}$$

where T_m is the motor torque, b is the viscous coefficient and c is the Coulomb torque, sometimes also said the static torque. Since the wheel's DC motor characteristics are unknown, a simple solution is to assume that the motor torque is proportional to the applied electric current and then

$$T_m = k_m \, I, \tag{7}$$

in which k_m is the motor constant and I is the current. Those equations are valid whenever the wheel is rotating, that is, $\omega_w \neq 0$. If the wheel's is in rest, the Coulomb torque shall be slightly changed in order to accommodate a current dead zone around null speed, which leads to

$$\dot{\omega}_w = \begin{cases} \dfrac{k_m I - b\omega_w - c\,\text{sgn}(\omega_w)}{J_r} - \dfrac{T_d}{J_p}, & \text{if } \omega_w \neq 0 \\[3mm] \dfrac{k_m I}{J_r} - \dfrac{T_d}{J_p} - c\,\text{sat}\left(\dfrac{k_m I}{c J_r} - \dfrac{T_d}{c J_p}\right), & \text{if } \omega_w = 0 \end{cases} \tag{8}$$

and sat(·) is the saturation function, defined by

$$\text{sat}(x) = \begin{cases} x, & \text{if } -1 < x < 1 \\ -1, & \text{if } x \leq -1 \\ 1, & \text{if } x \geq 1 \end{cases}. \tag{9}$$

This means that the wheel would not start to rotate unless the applied torques (motor and disturbance) are greater than the static torque. The kinematics of the single axis table is quite simple, and can be stated as

$$\dot{\theta} = \omega, \tag{10}$$

which shall be numerically integrated by the attitude estimator. Fig. 4 presents the block diagrams in Laplace transform for both the air-bearing table and the reaction wheel. In [4] a more detailed diagram of this reaction wheel was presented, including the friction torque, and in [17] the friction coefficients (static and viscous) were estimated by least squares (statistical) and deterministic methods. In this work the statistical coefficients were adopted; they are shown in Table 1, together with other parameters of the wheel and the air-bearing table. The input for the RW dynamic model is the current, and therefore this is the current control mode.
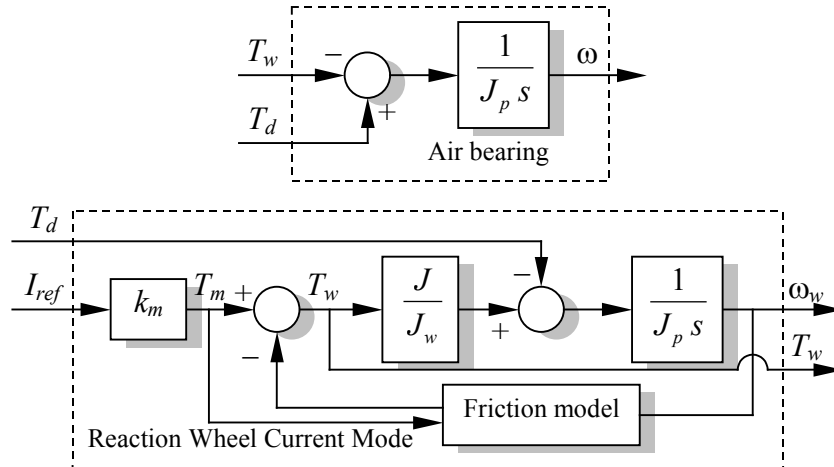

Figure 4: Air-bearing table and reaction wheel block diagrams.

RW Speed Control Loop

The RW uses a built-in PI (Proportional-Integral) controller so as to adjust its current based on the error between the required and the measured wheel's angular velocity, as can be seem in Fig. 5. The

Speed Control Mode is achieved by command that establishes the reference to the angular rate, while a command with a desired motor current assigns the RW to operate in Current Control Mode.

Table 1: Wheel and air-bearing table estimated parameters.

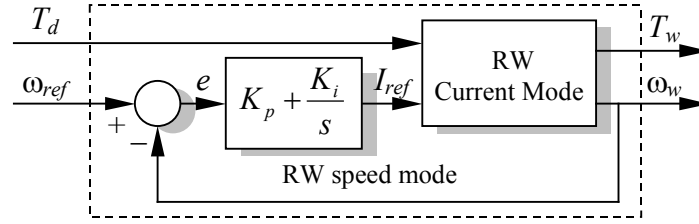| Parameter	Symbol	Value
Viscous coefficient	b	4.83×10^{-6} [N m s]
Coulomb torque	c	0.8795×10^{-3} [N m]
Motor constant	k_m	0.0228 [N m/A]
Wheel's inertia	J_w	1.5×10^{-3} [kg m^2]
Platform inertia	J_p	0,4954 [kg m^2]

Figure 5: Reaction Wheel speed control loop.

The SCM controller can be represented by

$$I_{ref}(t) = K_p\, e(t) + K_i \int_0^t e(t)\, dt,$$ (11)

where K_p and K_i are the proportional and integral gains, $I_{ref}(t)$ is the required reference to the motor current and the error $e(t)$ is computed as the difference $e(t) = \omega_{ref} - \omega_w$. In the discrete time domain, by applying the **z**-transform to the above relationship, one has

$$I_{ref}(k) = I_{ref}(k-1) + K_1\, e(k) - K_2\, e(k-1),$$ (12)

in which $e(k)$ is the error at time t_k, $k = 0, 1, ...,$ $K_1 = p\,(K_p + K_i\,\Delta t)$, $K_2 = -p\,K_p$, Δt is the time interval between sequential measures, and p is a proportional constant equals to 10723 rd/s/A, or 102.4 rpm/milliamperes, according to the RW interface document. The internal PI gains are $K_1 = 2000$ and $K_2 = -1900$ according with the same document, although they can be changed by command.

A second Speed Control loop was implemented in an external computer, in contrast to the built-in or internal SCM controller that resides in the RW/FOG electronics, and both were compared with respect to response to a command and performance. The discrete time interval for both the sensor measuring (FOG and RW speed) and the control loop was adopted as 0.2 s, although the maximum rate to send a command or to read the telemetry of the RW electronics is 10 Hz. At this rate the real time condition of the controller was no longer achieved, probably due to protocol communication lag. By fixing the external computer on the air-bearing table this problem can be solved. At the time of this writing that solution in being implemented.

A 1000 rpm reference speed was commanded to the RW and the results are shown in Fig. 6, for the external and internal control loops. It can be noted that the internal controller presents a better performance when compared to the external one, although the difference in the setting time is small. That is expected since the internal control probably uses a shorter sampling and control time interval. However the Bode diagram of both controllers, shown in Fig. 7 (amplitude) and Fig. 8 (phase), are similar, except for the phase angle, in which the external control appears to be a little bit better. Those diagrams where obtained by commanding the RW with a sinusoidal 1000 rpm

amplitude reference speed in open-loop, for both internal and external controllers. It is worth to mention that the frequency range that the RW is subjected when it is in normal orbit operation is less than 0.01 Hz (typically it is the magnitude of the orbital period, around 100 minutes), if one considers that the high frequency noise coming from the sensors is filtered. Therefore the small phase margin favouring the external control at high frequencies cannot be considered as an advantage.

Air-bearing attitude control

A conventional Current Mode PID controller was implemented in the off-platform computer so as to provide a way to compare the performances of the Current Mode and the Speed Mode controllers. The PID current controller was presented in [4] which showed that the maximum attitude deviation of the platform during RW reversal was almost 2 degrees, while this error remains below 0.05 degrees when the wheel is far from zero speed. That discrete controller was calculated by

$$u(k) = k_p \ e(k) + k_d \ \omega_g(k) + k_i \sum_{i=0}^{k} e(k) \Delta t , \qquad (13)$$

where the attitude error $e(k)$ is computed by

$$e(k) = \sum_{i=0}^{k} \omega_g(k) \Delta t , \qquad (14)$$

for a null reference attitude, and the adopted sampling time interval was 0.2 seconds. In this equation $\omega_g(k)$ is the FOG measure at time $t_k = k \ \Delta t$, $k = 0, 1, 2, \ldots$, already corrected by the gyro bias and the Earth's rotation rate, that estimates the air-bearing table angular speed ω. The gains were adjusted by trial, in order to have a minimum setting time with an over damped response to an impulse, and are $k_p = 0.04$ A/deg, $k_d = 0.2$ A s/deg and $k_i = 0.001$ A/deg s. For the Current Control Mode the reference current is given by the control signal u, that is, $I_{ref}(t) = u(t)$.
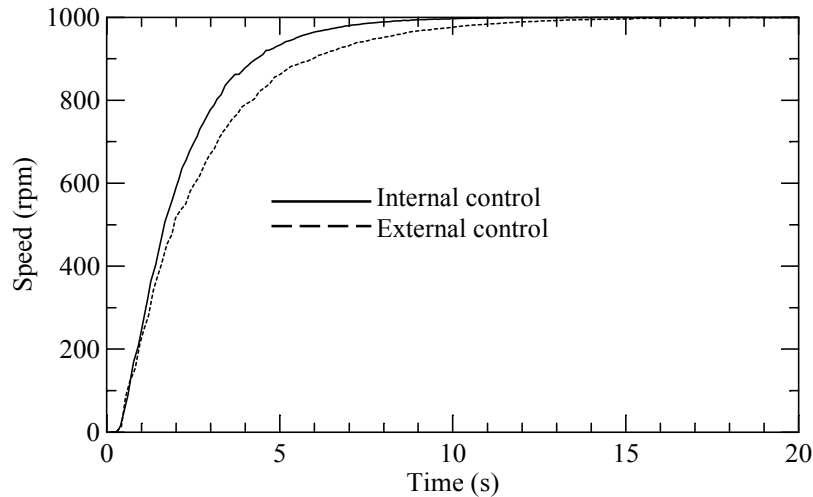

Figure 6: Step response of the RW for the internal and external controller.

To derive the speed control law, one starts with the Eq. (7) that relates the motor torque with the motor current. By the other hand, getting the discrete version of Eq. (2), it yields

$$\Delta \omega(k) + \Delta \omega_w(k) = T_w(k) \frac{\Delta t}{J_w} . \qquad (15)$$
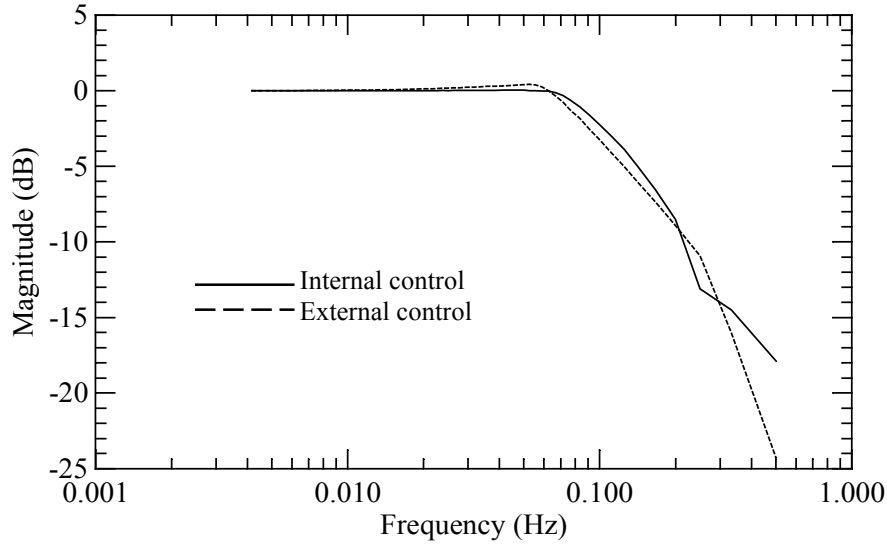
Figure 7: Bode diagram of the RW for both speed controllers: internal and external.
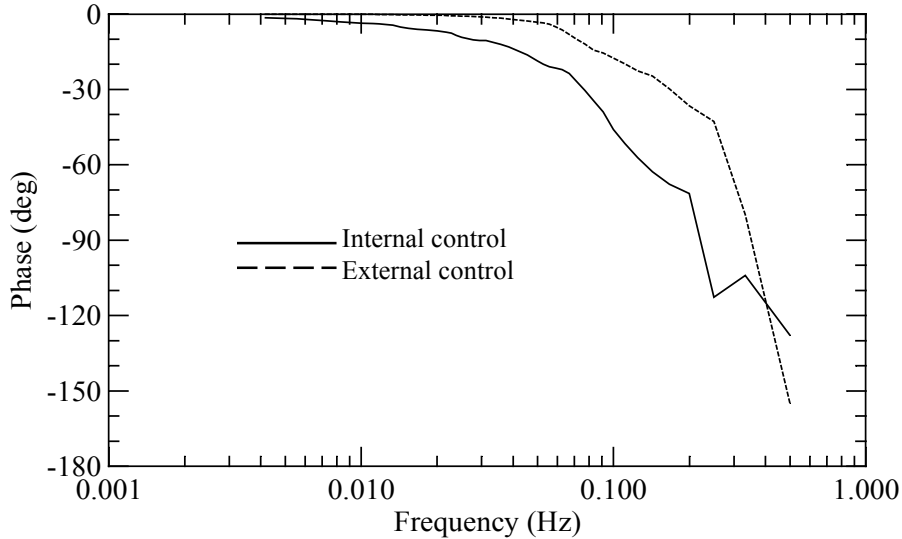

Figure 8: Phase angle of the RW for the internal and external speed controllers.

By assuming now that the platform acceleration $\Delta\omega(k)/\Delta t$ is negligible when compared to the wheel acceleration, and that the RW net torque T_w can be approximated by the motor torque T_m, then the reference wheel speed at time t_k can be calculated from the last expression, giving

$$\omega_{ref}(k) = \omega_{ref}(k-1) + \frac{k_m \, \Delta t}{J_w} I(k).$$ (16)

If now the current I is adopted as the signal control u, that is $I(k) = u(k)$, both the speed and current controllers shall present a similar steady state performance, although with noticeable different behavior during the wheel's sense reversal. The block diagram of the Speed Mode attitude control is shown in Fig. 9. Since there is no angular attitude sensor, the gyro data shall be integrated in order to provide the angular measurements. A simple mean filter on the gyro measures was implemented in the external controller, in order to avoid control instability due to the FOG noise. However this mean filter, based on a simple mean of the 3 last measurements showed small improvement since the high air bearing inertia acts already as a low pass filter.
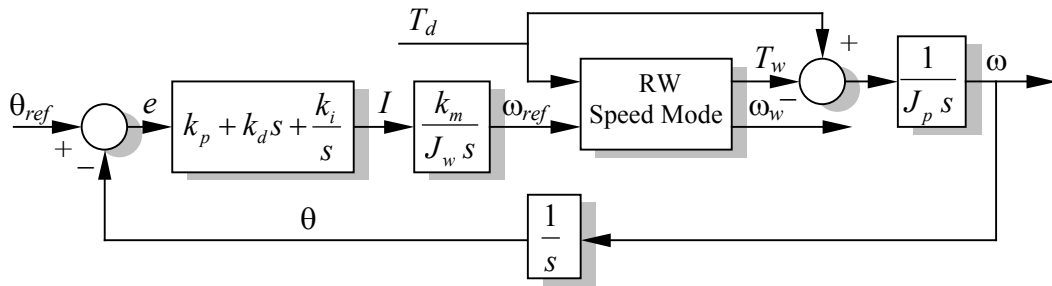
Figure 9: Block diagram of the air bearing attitude control with speed mode RW control.

The main result from the controller test is presented in Fig. 10. The RW started with −100 rpm and due to the fan torque the controller speeds up the wheel, in order to compensate for it. This torque can be estimated from the gradient curve of the angular speed, and resulted 4.4×10^{-4} Nm and 4.0×10^{-4} Nm for the external and internal speed control, respectively. This torque is two orders of magnitude higher than the environmental torques found in orbit. The wheel reverts its rotation sense at 35.2 and 37.4 seconds, which are clearly seen in Fig. 10, that shows the attitude error. Just after the zero-speed crossing the error starts to increase caused by the non-linear friction, but remains below a reasonable maximum error of 0.01 degree. When compared with the current mode control the difference is remarkable: more than 20 times lower. It is still to be analyzed the impact of the magnitude of the disturbance torque on the error, since the fan torque is far larger than the usual orbital torques, and the stability of the error rate during the wheel's reversal.

Fig. 11 shows the reaction wheel angular rate, as obtained by the RW telemetry. From the curves it is easy to see that the fan torque is practically constant, and from the conservation of the angular momentum the torque can be estimated by the slope, in accordance to Eq. 2, resulting 0.79×10^{-3} Nm for the external control and 0.71×10^{-3} Nm for the internal control. This magnitude is at least two orders of magnitude larger than the perturbing torques on small satellites in low Earth orbits.
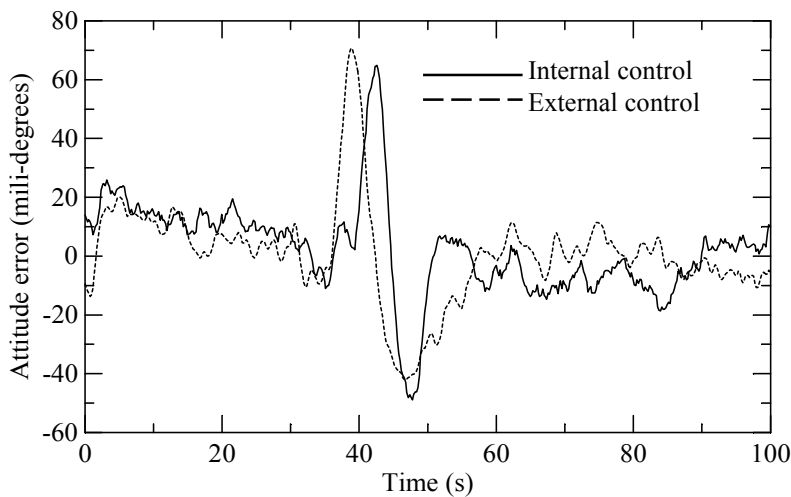

Figure 10: Attitude error of the air-bearing table with speed mode control.

Conclusions

This work presented experimental results of an air-bearing table attitude control with FOG gyro, a reaction wheel and a small fan employed to generate a disturbance torque. The reaction wheel dynamic model, including the bearing friction, was obtained and was characterized by means of step response and Bode diagram for speed mode control. The block diagram for both current and speed mode control was derived. A second speed mode control similar to the one found in the wheel drive electronics was implemented in an external computer and compared by means of the attitude control

performance during the wheel's rotation sense reversal for both controllers, internal and external. This was intended so as to get design knowledge base for a future RW development. The results have shown that the controllers have similar performance, as expected, but there is still some margin for performance improvements, like a predictive model control that includes the dynamic model of the reaction wheel, for instance. The maximum air-bearing table attitude error remained below 0.08 degrees with no filtering, which complies with fine attitude pointing stability of small satellites for Earth observations. The performance of the controller was also satisfactory, since the main attitude control of a satellite normally operates at 2 Hz, while the external control operated at 10 Hz. However it should be mentioned that the hardware was based on a PC (notebook indeed) that presents a higher performance when compared to a commercial space qualified on-board computer.
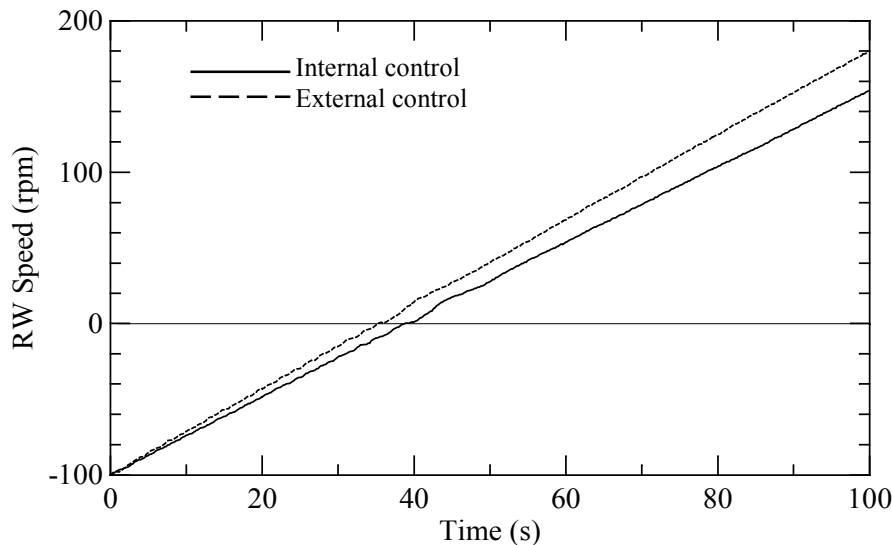

Figure 11: Reaction wheel angular rate in speed mode control

References

[1] J. R. Wertz, Spacecraft attitude determination and control (Astrophysics and Space Science Library), London, D. Reidel, 1978.

[2] V. Carrara and P. G. Milani, Control of one-axis air bearing table equipped with gyro and reaction wheel (In Portuguese), Proceedings of V SBEIN – Brazilian Symposium on Inertial Engineering. Rio de Janeiro, Brazil, Nov. (2007).

[3] V. Carrara, Comparison between means of attitude control with reaction wheels (In Portuguese), Proceedings of VI SBEIN - Brazilian Symposium on Inertial Engineering. Rio de Janeiro, Brazil, Nov. (2010).

[4] V. Carrara, R. Siqueira, D. Oliveira, Speed and current mode strategy comparison in satellite attitude control with reaction wheels. Proceedings of COBEM 2011 – 21st Brazilian Congress of Mechanical Engineering. Natal, RN, Brazil, Oct. (2011).

[5] M. L. B. Moreira, R. V. F. Lopes and H. K. Kuga, Estimation of torque in a reaction wheel using a Bristle model for friction, Proceedings of 18th International Congress of Mechanical Engineering, Ouro Preto, Brazil, Nov. (2005).

[6] S. S. Ge and H. Cheng, A Comparative Design of a Satellite Attitude Control System with Reaction Wheel. Proceedings of the First NASA/ESA Conference on Adaptive Hardware and Systems – AHS'06 (2006). (ISBN 0-7695-2614-4/06).

[7] H. Olsson, K. J. Åström, C. Canudas de Wit, M. Gafvert and P. Lischinsky, Friction models and friction compensation, European Journal of Control, Vol. 4, No. 3 (1998) 176-195.

[8] C. Canudas de Wit and S. S. Ge, Adaptive friction compensation for system with generalized velocity/position friction dependency, Proceedings of the 36th Conference on Decision and Control, San Diego, CA, Dec. (1997) 2465-2470

[9] C. Canudas De Wit, H. Olsson, K. J. Åström and P. Lischinsky, A New Model for Control of Systems with Friction, IEEE Transactions on Automatic Control, Vol. 40, No. 3 (1995) 419-425.

[10] C. Canudas De Wit and P. Lischinsky, Adaptive Friction Compensation with Partially Known Dynamic Friction Model, International Journal of Adaptive Control and Signal Processing, Vol. 11 (1997) 65-80.

[11] K. J. Åström and C. Canudas de Wit, Revisiting the LuGre Friction Model, IEEE Control Systems Magazine, Dec. (2008) 101-114.

[12] V. Carrara, A. G. Silva and H. K. Kuga, A Dynamic Friction Model for Reaction Wheels. Advances in the Astronautical Sciences. Vol 145. 1st IAA Conference on Dynamics and Control of Space Systems – DyCoSS'2012. Porto, Portugal, March (2012).343-352. (ISBN 978-0-87703-588-6).

[13] D. Karnopp, Computer simulation of slip-stick friction in mechanical dynamic systems. Journal of Dynamic Systems, Measurement, and Control, Vol. 107, No. 1 (1985) 100–103.

[14] F. Al-Bender, V. Lampaert and J. Swevers, The Generalized Maxwell-Slip Model: A Novel Model for Friction Simulation and Compensation. IEEE Transactions on Automatic Control, Vol. 50, No. 11, Nov. (2005).

[15] R. M. Hirschorn and G. Miller, Control of nonlinear systems with friction. IEEE Transactions on Control Systems Technology, Vol. 7, No. 5 (1999) 588-595.

[16] E. Oland and R. Schlanbusch, Reaction wheel design for cubesats. 4th International Conference on Recent Advances in Space Technologies, 2009. RAST'09., IEEE (2009) 588-595.

[17] V. Carrara and H. K. Kuga, Estimating friction parameters in reaction wheels for attitude control. Mathematical Problems in Engineering, Vol. 2013, p. 1-8, 2013. doi: /101155/2013/249674.